Pergamon

Int. J. Heat Mass Transfer. Vol. 40, No. 12, pp. 2825–2842, 1997

Printed in Great Britain
0017–9310/97 $17.00+0.00

PII: S0017–9310(96)00340–7

Some aspects of the modelling of wood chips drying in superheated steam

CHRISTIAN FYHR and ANDERS RASMUSON†

Department of Chemical Engineering Design, Chalmers University of Technology, S-412 96 Gothenberg, Sweden

(*Received* 10 *November* 1995 *and in final form* 16 *September* 1996)

Abstract—A comprehensive two-dimensional model is used to simulate the drying of wood chips in superheated steam. Emphasis is put on the drying conditions present in a pneumatic conveying dryer, i.e. high heat transfer rates and pressures. The internal mass transfer for these conditions limits the drying rate and, for a successful dimensioning of such dryer, not only the conditions inside the dryer but also the mechanisms occurring inside the single chip must be well understood. Wood chips of different sizes and species are studied. The effect of varying inlet temperatures of the chips (preheating), as well as the flashing effect at the outlet when the pressure drops (postdrying), are investigated. Different design parameters, such as the value of the heat transfer coefficient and the necessity of a two-dimensional model for the single wood chip, are also discussed. © 1997 Elsevier Science Ltd.

1. INTRODUCTION

Drying is often performed by allowing hot gas to come into contact with moist material, whereby heat is transferred to the surface of the material by convection. The heat evaporates water which, in turn, enters the gas stream. The most common drying medium is air, although the use of superheated steam is increasing. Energy recovery through the reuse of latent heat is simplified by the use of superheated steam, since the surplus steam may be condensed. Although this is the main benefit of this drying medium, the inert atmosphere is often advantageous for drying flammable materials or food products where the effect of sterilization is important [1].

One aspect in the modelling of dryers which is often overlooked is the transport mechanisms occurring within the material during the drying process. Much effort is often put into the prediction of the conditions in the dryer; drying is often assumed to be unhindered or else some simple drying model is applied. For the successful prediction of the performance of a certain dryer, however, both the conditions inside the dryer as well as the transport mechanisms within the single particle must be well understood. This paper deals with some aspects which are affected by the internal transport mechanisms in a single wood chip. The ultimate aim for the present research is to develop a complete model for a pneumatic conveying dryer. The external conditions in which the single particle is dried, therefore, reflects the conditions in such a dryer.

† Author to whom correspondence should be addressed.

2. MODEL

A model for drying porous, anisotropic materials with specific application to wood, has been developed recently [2]. The work was based on the drying of wood chips, although the model can be used for the drying of other hygroscopic porous materials with relevant sets of material data.

2.1. *Theoretical*

The dimensions of the wood chip upon which the simulations and experiments were based are depicted in Fig. 1. The chip is treated as being stationary with steam flowing past as indicated. Three different points are denoted in the figure: point 1 is located on the edge, point 2 is located at the small surface perpendicular to the longitudinal direction and point 3 is located in the centre of the chip.

Three moisture phases were accounted for: free (liquid) water, bound water and water vapour. The model is two-dimensional (transversal and longitudinal directions) and treats the coupled flow of water, air and steam by an extended Darcy's law. The diffusion of bound water is modelled by a Fick law expression. The complete set of transport equations and balance equations are given in the Appendix. Heat is transported internally by convection and conduction whereas external heat transfer to the surface occurs via convection and radiation. The model can cope with a wide range of external conditions such as high temperatures and steam pressures above the atmospheric. A code written for geothermal applications developed by Pruess [3] at Lawrence Berkeley Laboratories formed the basis for this work. The code

NOMENCLATURE

C_p	heat capacity [J kg^{-1} °C]
D	diffusion coefficient [m^2 s^{-1}]
H	heat accumulation [J m^{-3}]
H	enthalpy [J kg K^{-1}]
h	heat transfer coefficient [W m^{-2} K^{-1}]
j_D	Chilton–Colburn factor for mass transfer
j_H	Chilton–Colburn factor for heat transfer
K	absolute permeability [m^2]
L	length [m]
k	relative permeability
k_c	mass transfer coefficient [m s^{-1}]
M	molar mass [kg kmole^{-1}]
n	mass flux [kg m^{-2} s^{-1}]
P	pressure [Pa]
Pr	Prandtl number
q	heat flux [J m^{-2} s^{-1}]
R	gas constant [J mole K^{-1}]
S	saturation
Sc	Schmidt number
T	temperature [K]
T	thickness [m]
u	internal energy [J kg^{-1}]
v	velocity [m s^{-1}]
W	mass accumulation [kg]
X	moisture content [kg/kg]
x	mass fraction
y	molar fraction.

Greek symbols

ε	porosity
λ	heat conductivity [W m K^{-1}]
μ	viscosity [kg m^{-1} s^{-1}]
ρ	density [kg m^{-3}]
σ	Boltzmanns constant [W m^{-2} K^{-4}]
σ	surface tension [N m^{-1}].

Subscripts

bw	bound water
c	capillary
c	convective
eff	effective
f	film conditions
fsp	fibre saturation point
g	gas
L	longitudinal direction
l	liquid
s	surface
sat	saturated
T	transversal direction
v	vapour
w	water
∞	surroundings.

Superscript

κ	component
w	water.

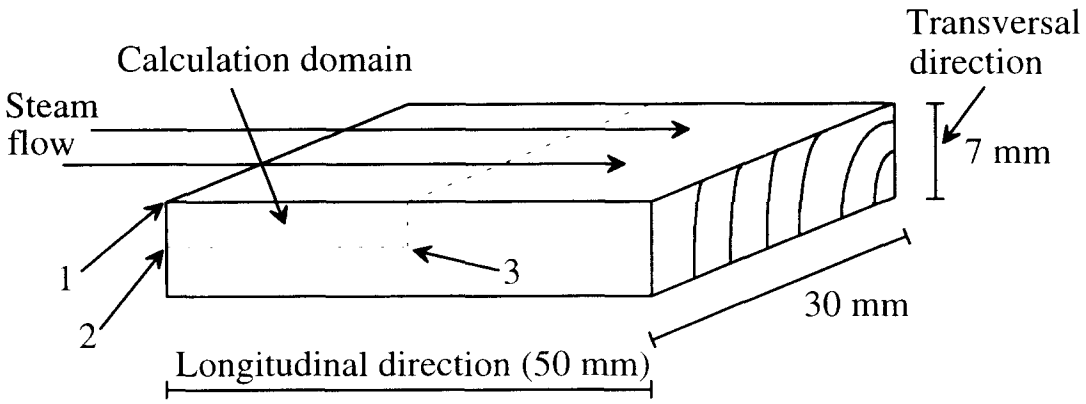

Fig. 1. Dimensions of the wood chip.

is called "TOUGH" and includes general features of transport in porous media and, with some modifications and extensions, it could be used to simulate the drying of wood.

2.2. *Experiments*

Experiments for the two most common softwoods (pine and spruce) at a wide range of external conditions were performed in order to validate the theoretical model [2]. The equipment enabled simultaneous measurements of the average moisture content as well as the temperature and pressure in the centre of the chip. All simulations were performed prior to the experiments and all transport parameters were taken from the literature. A comparison between the experiments and calculations showed good agreement. All experimentally observed physical features of the drying were predicted well by the simulations. Based on

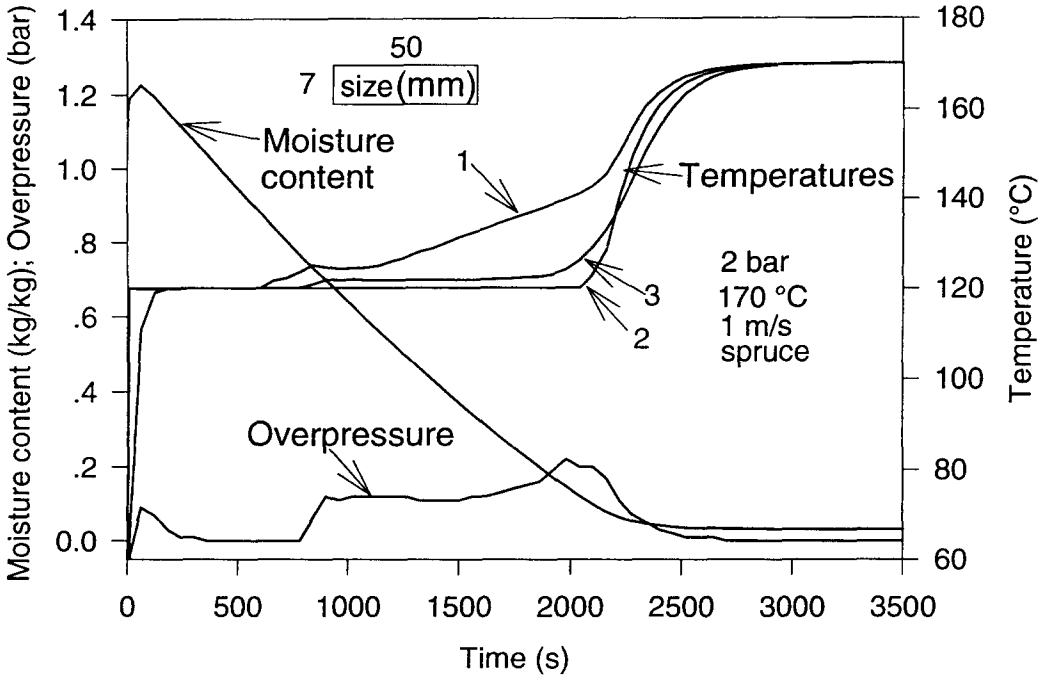

Fig. 2. General drying behaviour at 2 bar and 170°C.

this work it can be concluded that the model is sufficiently accurate in providing relevant drying predictions, even for conditions beyond the range of which the experiments were performed.

2.3. *General drying behaviour*

The general behaviour of drying spruce at 2 bar and 170°C is depicted in Fig. 2. The moisture content increases initially due to the condensation of steam on the surface as well as within the material. The initial pressure inside the particle is 1 bar, which means that the surrounding steam is forced into the chip where it condenses and increases the moisture content. The pressure is equalized in about 20 s. The overpressure at the centre of the material is also plotted in Fig. 2. The overpressure is a function of the temperature and, therefore, starts to rise simultaneously with the rise in temperature at the centre. The small initial overpressure during the first 100 s is due to the initial heating of the chip to the boiling point. The surface enters the hygroscopic range at about 700 s, causing the temperature and, accordingly, the pressure to rise throughout the material. The overpressure reaches the maximum value at about 1860 s and then declines as the moisture content falls below the X_{fsp}.

The temperature at three different points are also plotted in Fig. 2. The locations of these points are illustrated in Fig. 1. Point 1 is located at the edge of the chip, point 2 on the surface perpendicular to the longitudinal direction and point 3 in the centre of the material. The temperatures increase rapidly up to the boiling point and remain there during the period of constant drying rate. When the liquid transport at the surface is no longer sufficient to consume the transferred heat by evaporation, the temperature rises above the boiling point. Since point 1 is located at the edge, the temperature rises first at this point. Note that the temperature at point 2, although it is located on a surface, is held at the boiling point for a longer period of time than at point 3, which is located in the centre of the material. This indicates that the moisture content is higher at point 2 and is due to the internal overpressure which drives the moisture in the more permeable longitudinal direction, causing an accumulation of moisture at the small end. General drying behaviour is discussed at length by Fyhr and Rasmuson [2].

3. EFFECT OF DIFFERENT WOOD CHIP PROPERTIES

3.1. *The effect of permeability and different wood species*

The main difference between the two different groups of softwood species, pine and spruce, is the value of their absolute permeability. Pine wood has an internal structure which makes it more permeable than spruce. The difference in permeability, according to the literature, is about 1 to 2 orders of magnitude, depending on direction. The degree of anisotropy for spruce is expected to be larger than for pine. The ratio of earlywood to latewood in a tree also has significant effect on permeability. A fast-growing tree generally has a lower density due to a larger proportion of low-density earlywood. The earlywood tracheids have thinner cell walls, and the bordering pits are more numerous and greater in diameter than the latewood pits. This gives rise to greater initial water per-

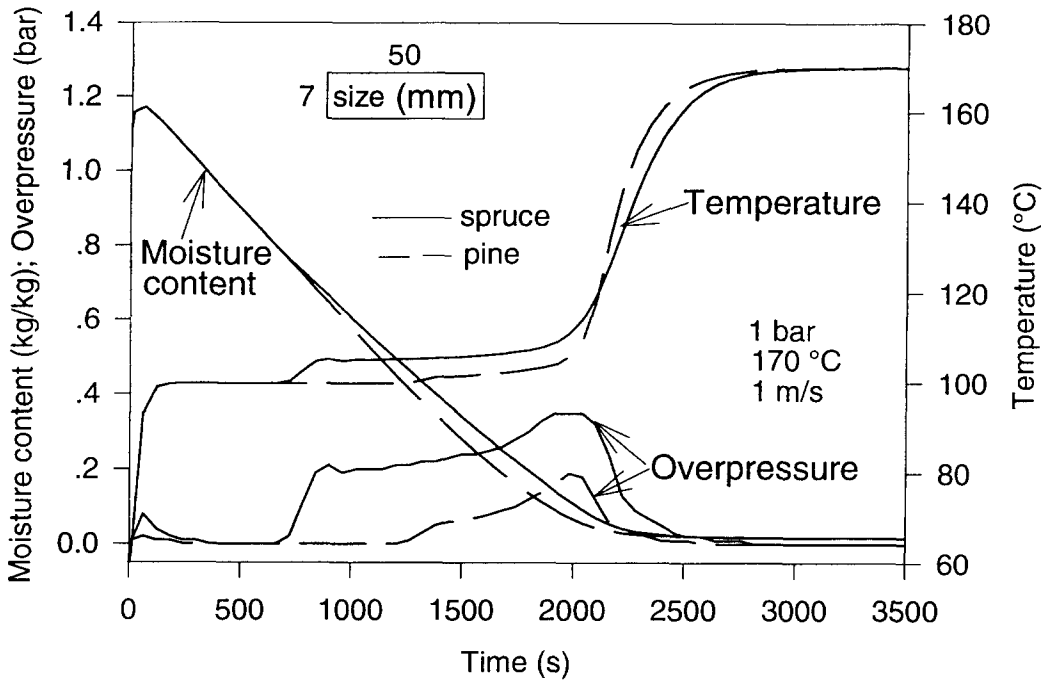

Fig. 3. Comparison of spruce and pine wood.

meability than for a latewood tracheid. A slow-growing tree contains more latewood tracheids with smaller and more rigid pits. The latewood pits, accordingly, have greater resistance to aspiration, and the permeability of dry latewood is usually higher than for dry earlywood. To summarize, the absolute permeability of the liquid phase is most often higher for wood of lower density but, due to its greater tendency to aspirate, the gas phase permeability is usually lower than for high density wood. The permeabilities for the transition region between wet and dry wood lie somewhere between. A linear relationship is, however, unlikely since the pit aspiration is dependent on the drying conditions and, in a complex manner, on the moisture content [4]. The effect of permeability on drying behaviour for drying at 1 bar and 170°C is depicted in Fig. 3. The total drying time is about 5% shorter for pine wood. The period of constant drying rate is longer for pine due to its higher permeability which allows the capillary forces to keep the surface above X_{fsp} for a longer time. Drying in the falling rate period is also faster for pine since the permeability in the longitudinal direction is greater than for spruce.

Fast growing trees have a higher porosity than slow growing trees, which results in that their initial moisture content is considerably higher than 1.2. Some extra runs were performed in order to determine the effect of porosity. The results for drying at 170°C and 1 bar with a porosity of 0.73 instead of 0.66 are shown in Fig. 4. The curves are similar to those for dense wood but the maximum overpressures are somewhat smaller. There is no visible plateau in the curve for the overpressure in pine, which is also an effect of its higher permeabilities. The initial overpressure is the same for both types of wood, which indicates that it is not affected by permeability. The fact that the magnitude of the maximum overpressure for pine is reduced to one third of that of spruce is mainly attributed to the higher permeability in the longitudinal direction. The difference in the temperature profiles is due mainly to the different distributions of moisture during the final part of the drying process. The last remaining moisture in spruce wood is located near the smaller surface (Fig. 7(c)) whereas the final moisture in pine wood is found in the centre of the wood chip, (Fig. 6(c)). The moisture content affects the heat conductivity, which causes a steeper temperature profile for pine. Experiments with soft pine and spruce were also performed in order to validate the theoretical discussion, and the results obtained are given in Fig. 5.

The difference in the drying curves is not as obvious in the experiments as in the calculations. This is at least partly due to a value which is somewhat too low for transversal permeability in the calculations. The shapes of the temperature curves match well, as the curve for pine is steeper in the final heat-up period in both figures. The ratios between the maximum overpressures are also in good accordance.

The different permeabilities also cause different evolutions of the moisture distributions. The moisture distributions for drying of pine and spruce at 2 bar and 170°C at three different times are depicted in Figs. 6(a–c) and 7(a–c). The three points denoted in Fig. 6(a) are the same as in Fig. 1. The distribution of pine at 660 s (6a) compared with spruce (7a) shows that the moisture gradients in the transversal direction are much smaller for pine. This is due to the higher per-

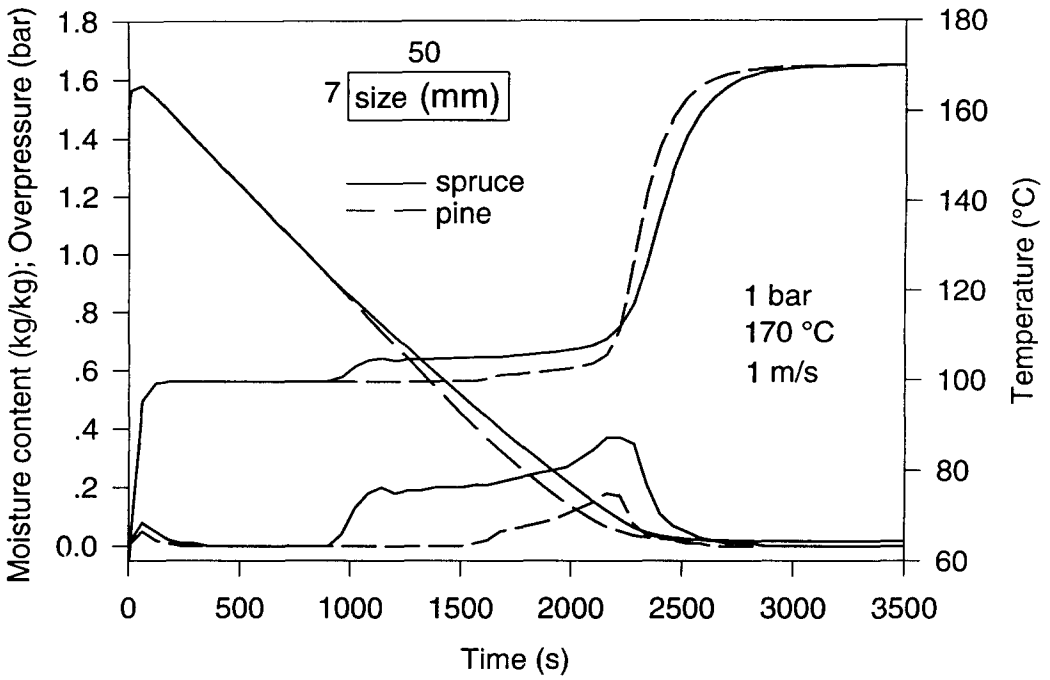

Fig. 4. Calculated drying behaviour of soft spruce and pine.

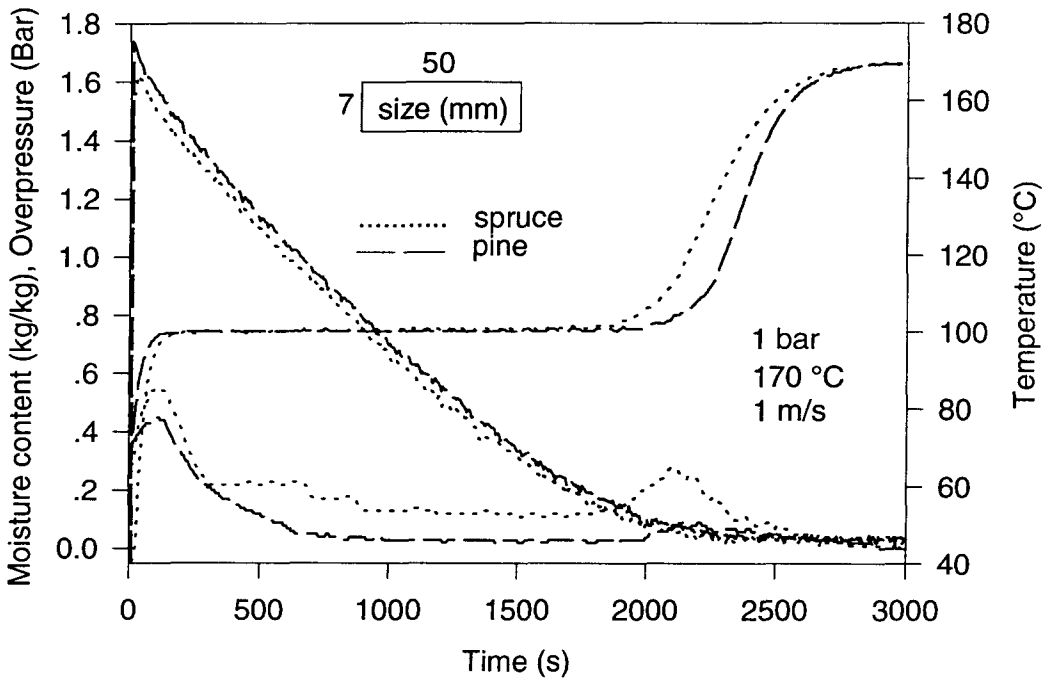

Fig. 5. Measured drying behaviour of soft spruce and pine.

meability of pine, which allows capillary action to distribute the moisture evenly. The higher permeabilities in both directions in pine wood also lead to a smaller overpressure and, consequently, less flow in the longitudinal direction. Less moisture is then accumulated at the small surface, as can be seen by comparing the distributions at 1200 s (Figs. 6(b) and 7(b)). The only remaining moisture for pine at 1860 s (6c) is located in the centre of the material and not at the surface, as is the case with spruce.

The effect of differences in permeability between different species on the drying time becomes more pronounced the more severe the drying conditions. In order to investigate this, additional runs with the velocity increased to 10 m s^{-1} were performed. This velocity is expected to be relevant for a pneumatic

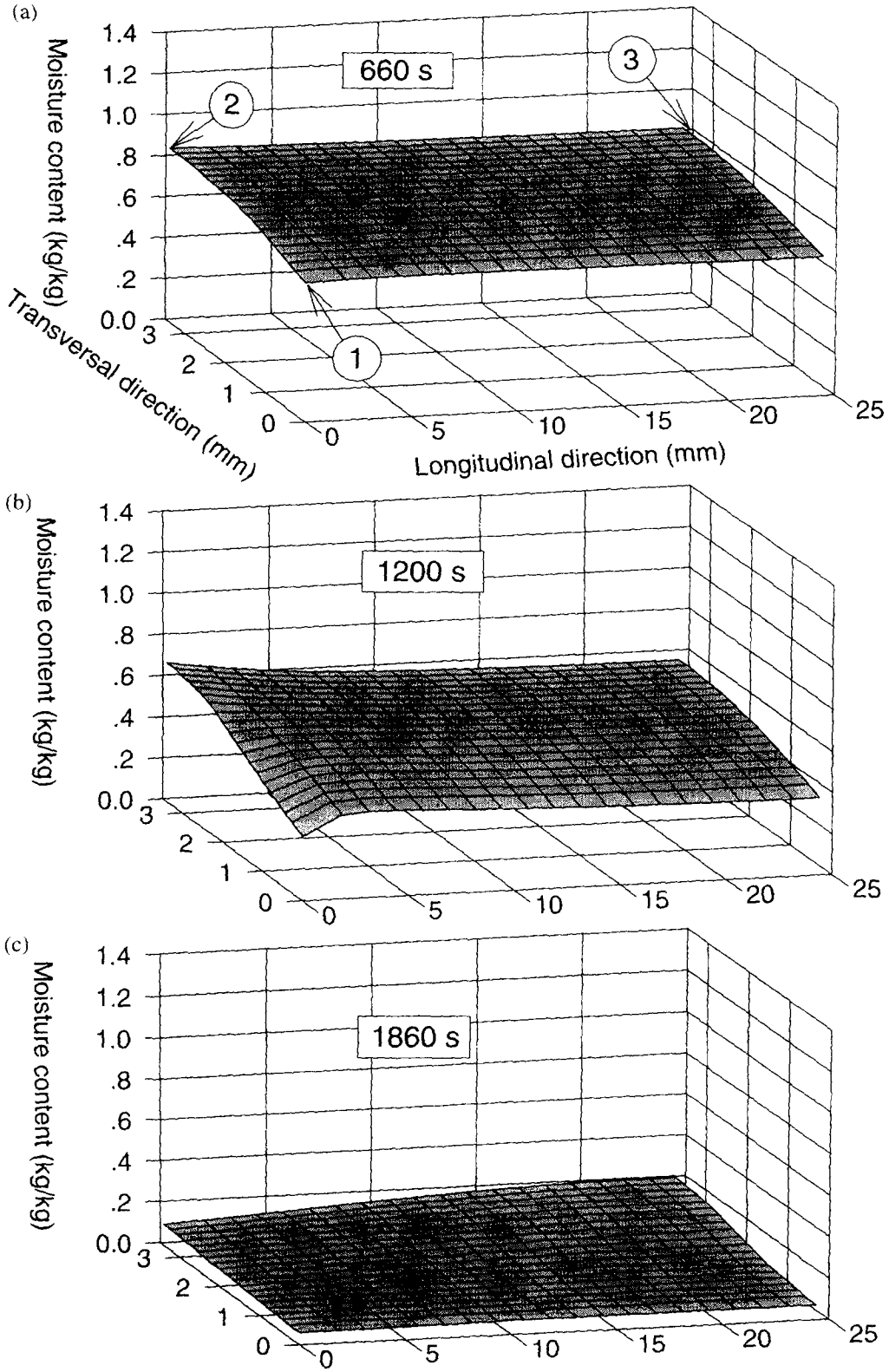

Fig. 6. Moisture distributions for pine at (a) 660; (b) 1200; and (c) 1860 s.

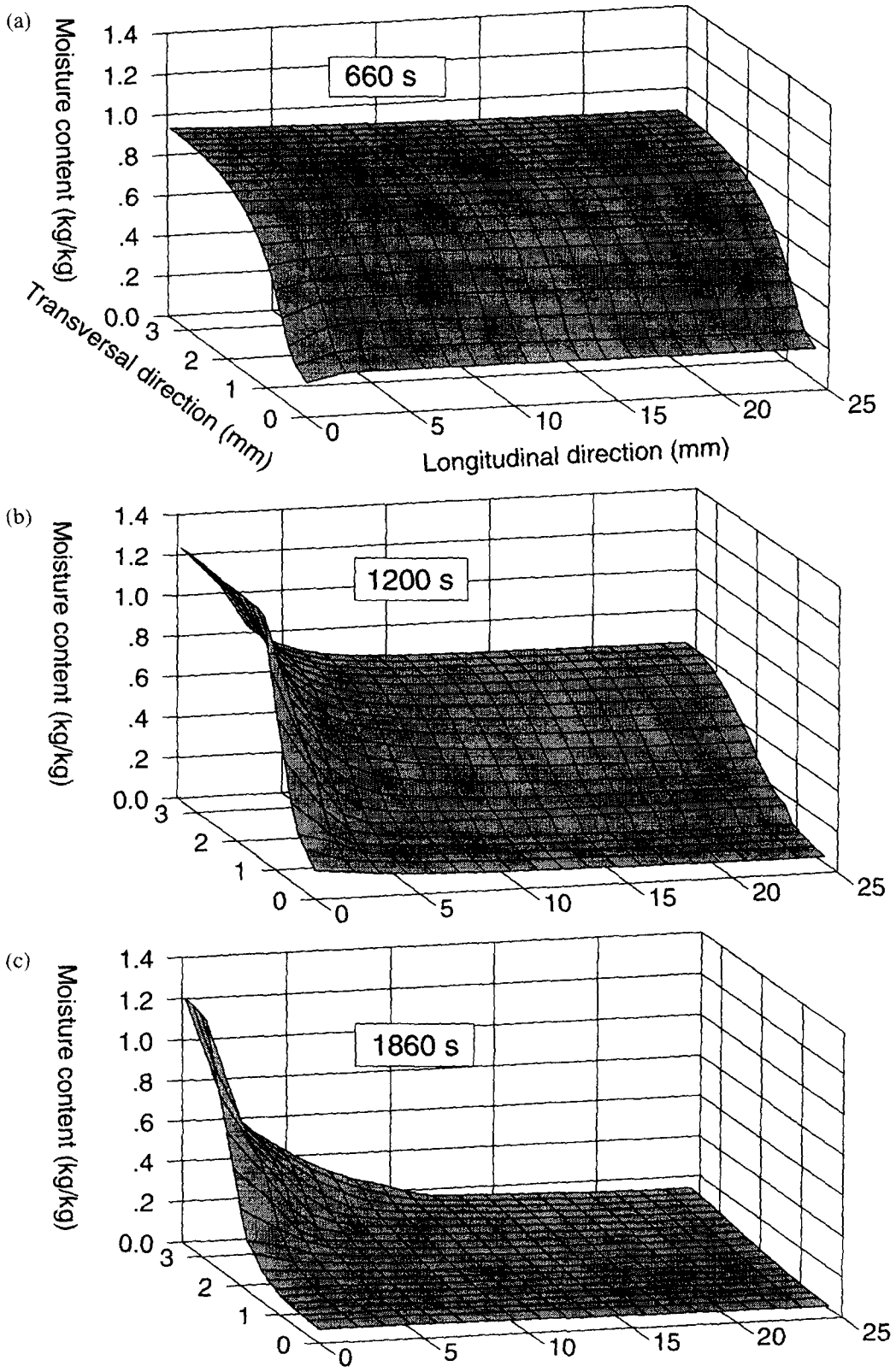

Fig. 7. Moisture distributions for spruce at (a) 660; (b) 1200; and (c) 1860 s.

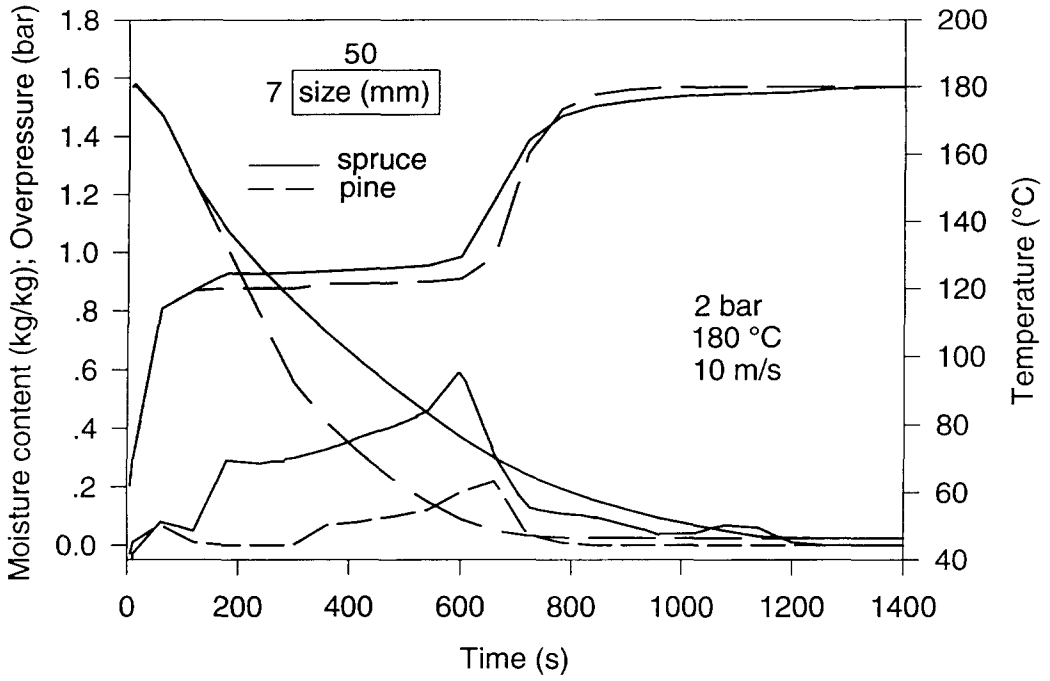

Fig. 8. Drying behaviour of spruce and pine under severe conditions.

conveying dryer and reflects the slip velocity between a chip and the steam. The resulting drying behaviours are depicted in Fig. 8.

The drying rates are, as expected, equal during the initial part of drying: after about 200 s, pine dries faster than spruce as the latter enters the falling rate period first due to its lower permeabilities. The total drying time then becomes considerably shorter for pine, as is exemplified by the fact that the drying time down to 0.2 in moisture content is about 60% longer for spruce. This leads to problems with mixed materials in a dryer since the exit moisture content differs considerably; it highlights the necessity of taking the properties of different types of materials into account.

3.2. *Effect of the geometry of the wood chips*

The length of real wood chips usually does not exceed 50 mm but, in order to investigate sensitivity to the change of length, two additional runs for spruce chips with $L = 25$ and $L = 100$ mm were performed. The same reasoning applies to the thickness of the wood chips which was also varied in the same manner.

Table 1. The influence of chip geometry on the drying

Length (mm)	Thickness (mm)	Max. over-pressure (bar)	Total drying time (s)
50 (ref.)	7	0.21	2880
50	14	0.15	6060
50	3.5	0.38	1440
100	7	0.66	3840
25	7	0.09	2280

Table 1 presents the results of drying in 2 bar and 170°C with the original dimensions as a reference.

Some general conclusions may be drawn despite the fact that the range of dimensions does not exactly match the real wood chips. It is clear from Table 1, that when the thickness is doubled, the total drying time is approximately doubled; the reverse is also valid when the thickness is halved. It is notable that the maximum overpressure in the centre of the material is greater for the thinner chip, the explanation for this being that the distance for the transport of heat from the surface to the centre is halved and that the main pressure release occurs in the longitudinal direction. When the longitudinal dimension is doubled, the maximum overpressure increases by a factor of more than two, this is due to the greater length of longitudinal flow necessary for pressure equalisation. The reverse is valid if the length is halved. The total drying time is not as sensitive to the wood chip length as to the thickness, the total time is affected only by a factor 0.75 when the length is halved. This is because the main input of heat, namely through the surface perpendicular to the transversal direction, increases or decreases in the same manner, even though the total volume of the wood chip changes. Based on this discussion, it may be stated that for equal volumes, a thin chip is better for drying purposes than a short one. Insofar as is practical, therefore, it is advisable to control the cutting process so that the chips produced have these geometrical features. The essence of this reasoning is that a reduction of the direction with the highest resistance to flow is the most effective way of shortening the drying time.

It was found in the simulations that an increase

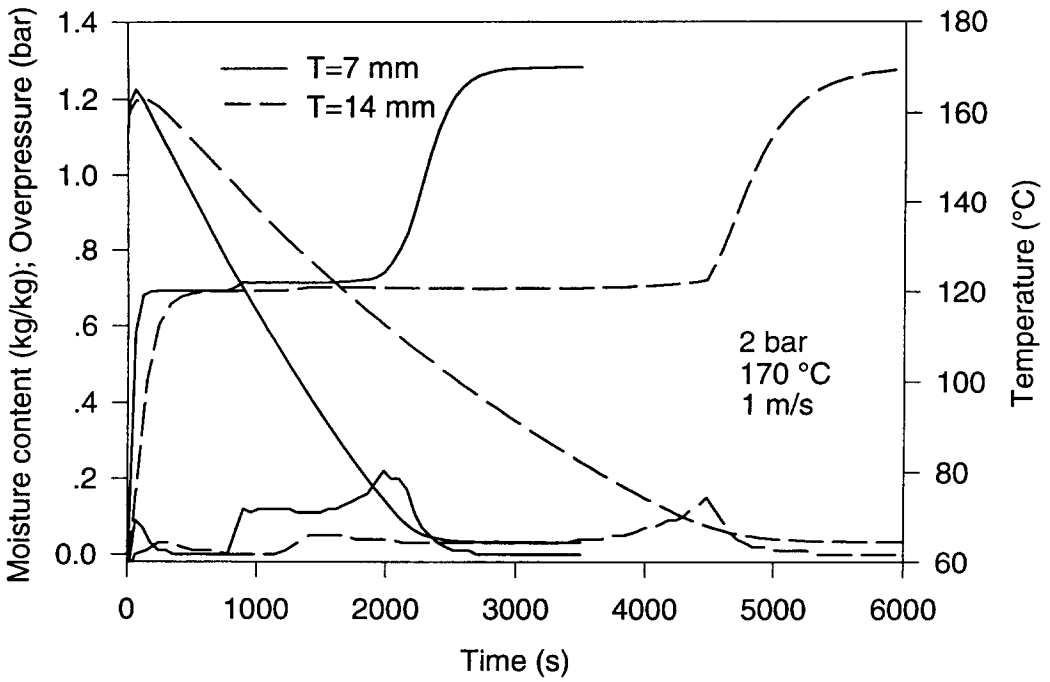

Fig. 9. Calculated effect of thickness.

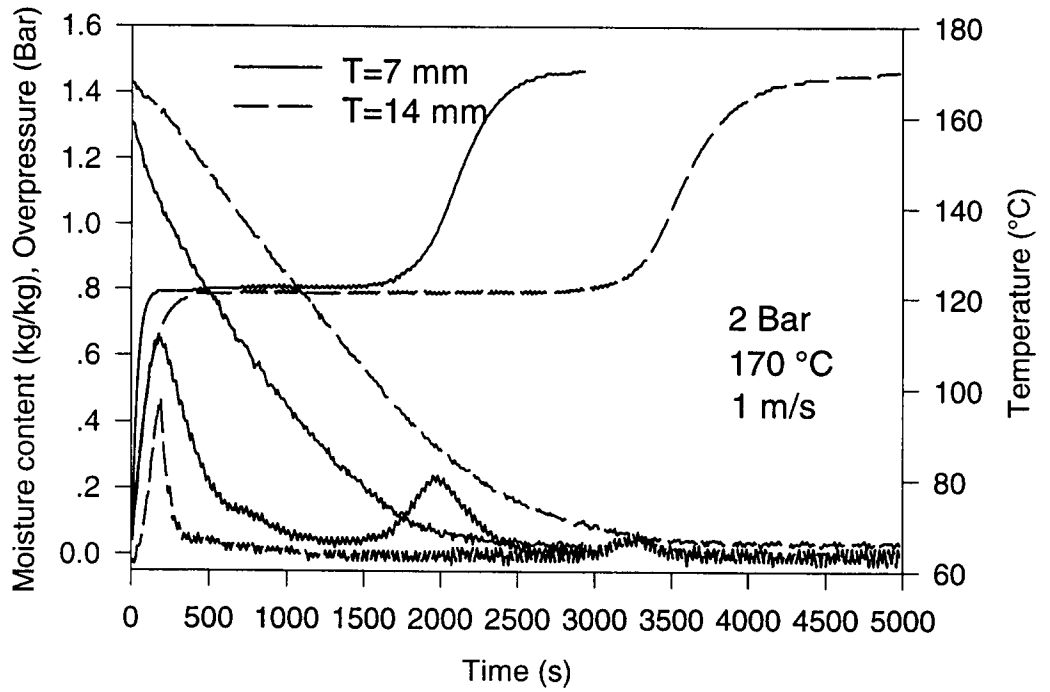

Fig. 10. Measured effect of thickness.

of the thickness more than doubled the total drying time and also, somewhat unexpectedly, reduced the maximum overpressure, as depicted in Fig. 9. Experiments with thicker spruce chips were performed in order to validate the simulated effect of geometry, the measured drying behaviour of the cases given in Fig. 9 is depicted in Fig. 10.

The predicted drying behaviour of the thick chip is verified by the experiments in the sense that the overpressure is clearly lower and the total drying time is approximately doubled. The temperature profiles during the heat-up period are very similar, which indicates that the intrinsic heat transport is predicted well. The total drying time for the thick chip ($T = 14$ mm)

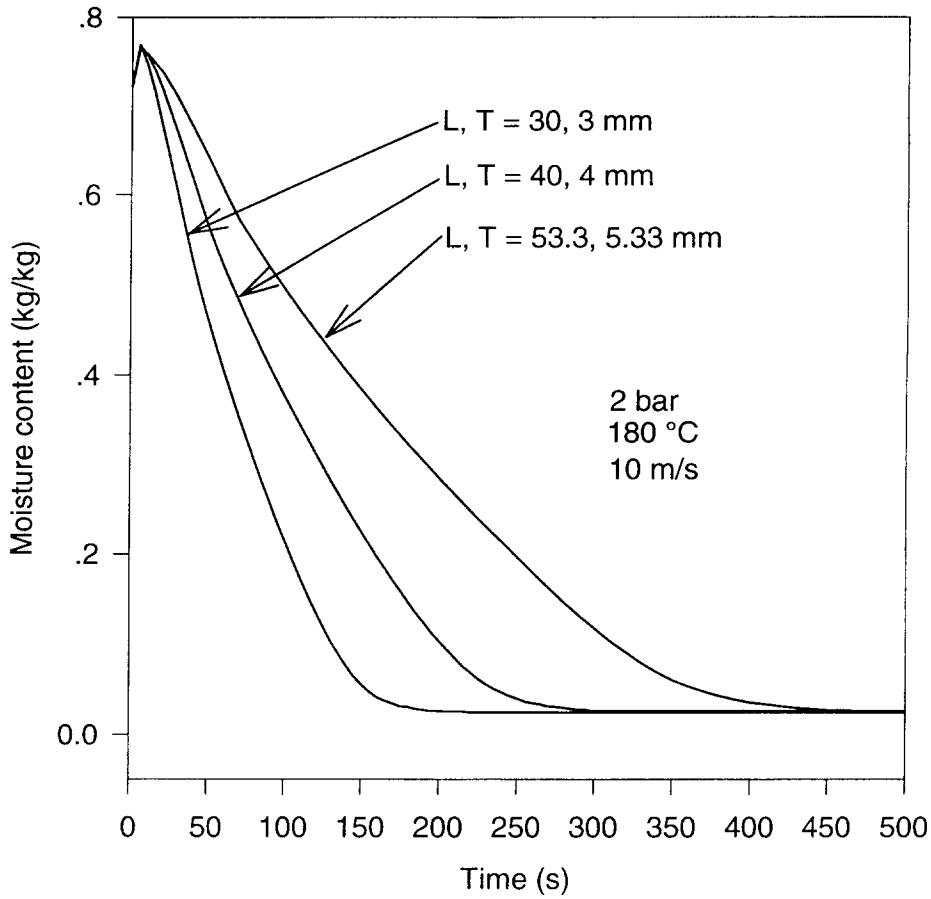

Fig. 11. Drying curves for different wood chip sizes.

is somewhat longer in the simulations, which can be explained by the relative increase of the surface perpendicular to the disregarded transport direction as the thickness increases.

The size and initial conditions of the chips used this far were chosen in order to simplify the comparison between the experiments and calculations. Wood chips, are, however, normally stored before drying, so a more realistic value of the initial moisture content is about 0.7. Wood chips from a cutting machine contain a wide range of sizes which, in turn, leads to different final moisture contents when dried under the same conditions given an equal residence time in the dryer. Three different chip sizes, obtained by scaling with a factor of 1.33 in both the longitudinal and transversal directions, were studied. Note that the different widths of the chips do not affect the results since this direction is not included in the model. The permeabilities for pine wood were chosen to be $K_T = 2.5 \times 10^{-16}$ m^2 and $K_L = 1.0 \times 10^{-12}$ m^2. The drying conditions reflect a pneumatic conveying dryer with a slip velocity equal to 10 m s^{-1} and superheated steam at 2 bar and 180°C. The resulting drying curves are depicted in Fig. 11.

Figure 11 shows that a large chip dries considerably slower than a small chip. It can be concluded from this figure as well as from Table 1 that the total drying time (TDT) approximately follows the following relation

$$TDT_1 = TDT_0 \frac{T_1}{T_0} \sqrt{\frac{L_1}{L_0}}. \quad (1)$$

That is, the total drying time increases linearly with increased thickness (T) and to the square root of the change in longitudinal length (L). The ratio of the total drying time for the largest chip to the smallest chip is, then, $5.33/3 * \sqrt{53.3/30} = 2.4$, which is in accordance with the curves in Fig. 11. Relation (1) is very accurate for pine wood; in the case of spruce the right hand side should be multiplied by a factor of about 1.3 in order to obtain the same accuracy.

The total drying times are still long in comparison with the residence time in a pneumatic conveying dryer (20–40 s). The convective heat transfer is modelled here, as if the wood chip is stationary and the steam flowing past as depicted in Fig. 1. However, chips flow in a very irregular manner in real dryers, which is expected to increase the convective heat transfer considerably. The slip velocity in a conveying dryer is considerably higher locally than 10 m s^{-1} due to

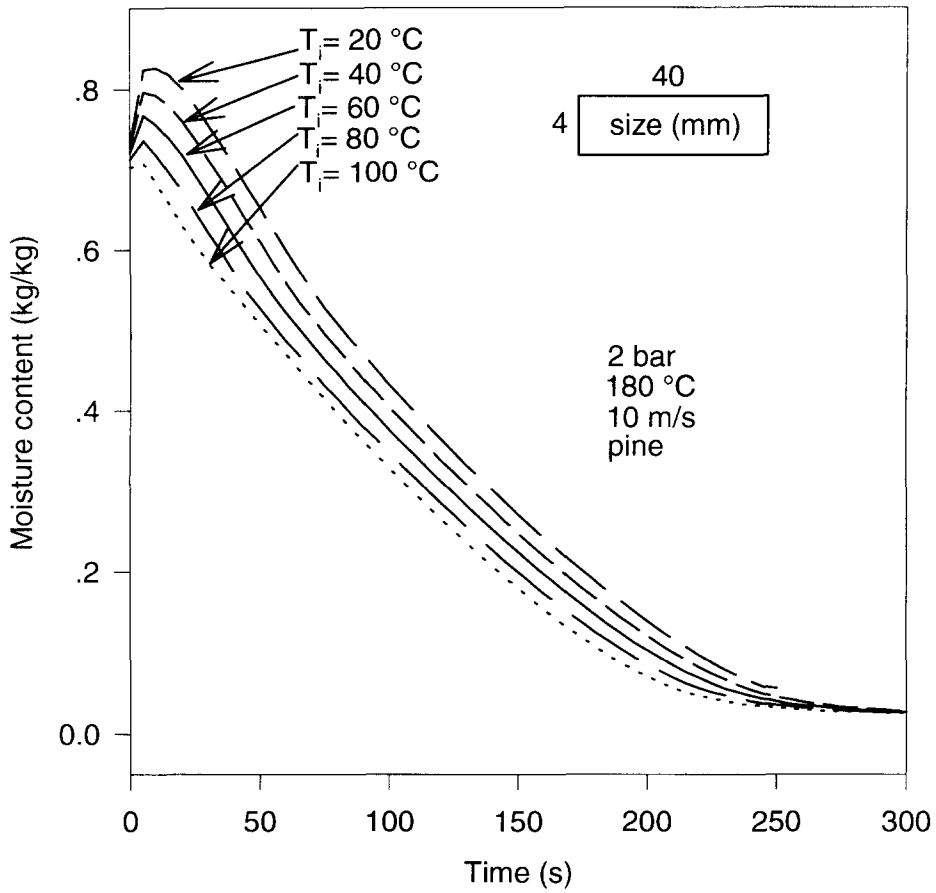

Fig. 12. The effect of preheating.

acceleration zones at the inlet and in pipe bends. Furthermore, the final moisture content is considered here as the equilibrium moisture content, whereas an exit moisture content of 0.2–0.3 kg kg^{-1} is sufficient for combustion purposes.

4. INLET AND OUTLET CONDITIONS

4.1. *Initial temperature: the effect of preheating*

It has been shown in the preceding calculations that condensation on the surface initially increases the moisture content. For the drying case in Fig. 11 where $L, T = 40$, 4 mm, the initial temperature is 60°C and the time required to reduce the moisture content to its original value is about 20 s. This, in turn, increases the total drying time by the same amount, which results in a poor utilization of the drying equipment. It is therefore favourable to preheat the chips before entering the dryer. In order to investigate the effect of preheating on the total drying time, the drying curves for five different initial temperatures between 20 and 100°C are compared in Fig. 12.

The somewhat different values of the initial moisture content are an effect of the different temperatures which lead to different liquid densities. The amount of condensation increases as the initial temperatures are lowered, just as expected. The negative effect of inserting chips at room temperature (20°C) is clearly seen since the moisture content is initially increased by about 15%, which increases the total drying time by about 50 s. The positive effect of preheating is more pronounced at the beginning of the drying which is exemplified by the fact that the difference in moisture content between the 20°C case and the 100°C case is about 0.15 at 50 s but only 0.09 at 150 s.

4.2. *Conditions at the outlet: postdrying*

The outlet, where the surrounding pressure suddenly drops to atmospheric, is another interesting part of the dryer. Flashing occurs if the particle still contains free water, which leads to very high drying rates. The external and internal diffusional mass transfer must be accounted for since the surrounding atmosphere is air after the outlet. The additional boundary condition then becomes:

$$\mathbf{n}_s^w = k_c M_w \frac{P}{RT}(y_g^{w,s} - y_g^{w,\infty}) \tag{2}$$

where k_c is the mass transfer coefficient obtained by analogy between heat and mass transfer according to Chilton–Colburn:

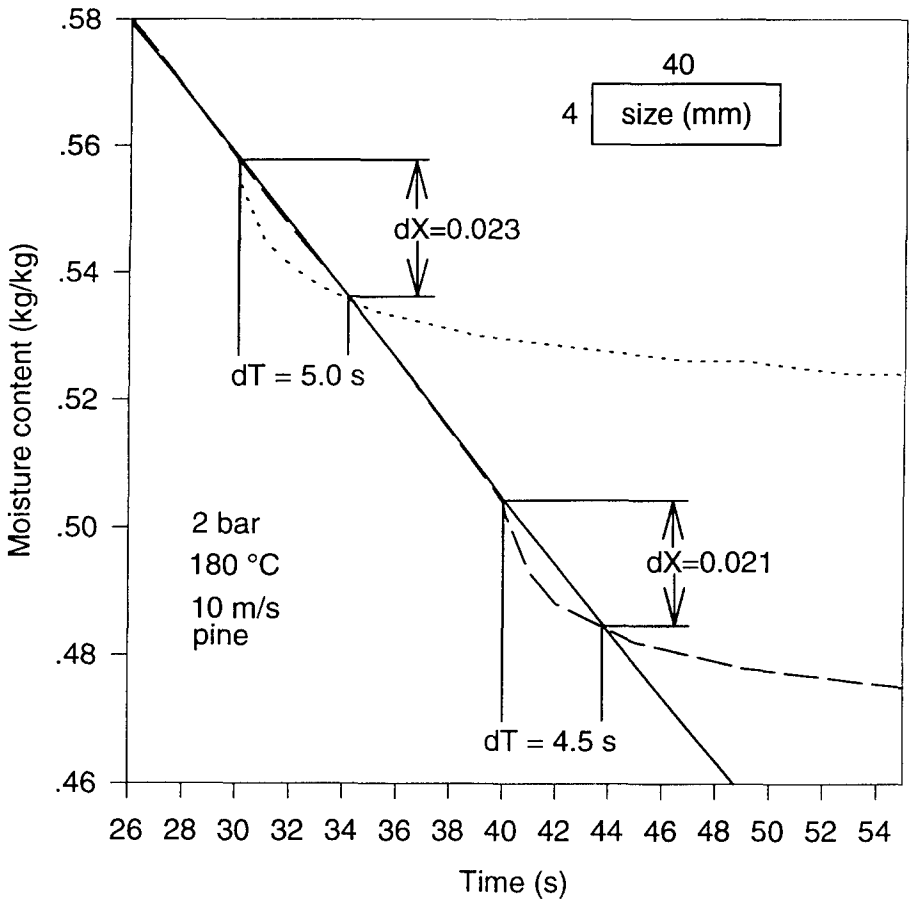

Fig. 13. The effect of post-drying.

$$j_D = j_H \Leftrightarrow \frac{k_c}{v_\infty} Sc^{2/3} = \frac{h}{c_p v_\infty \rho} Pr^{2/3}. \quad (3)$$

The internal diffusion of vapour in the gas phase is added as:

$$\mathbf{n}_g^w = -D_{eff} \nabla \rho_g^w. \quad (4)$$

A detailed investigation of the drying of wood chips in air has been made by Johansson *et al.* [5]. The effect of post-drying when the chips leave the dryer at two different times is depicted in Fig. 13. The conditions outside the dryer are set at air at 1 bar and 20°C and the slip velocity between the chips and air is set at 1 m s^{-1}, which is assumed to reflect the velocity of a conveyer belt.

The drying rates are initially very high due to the flashing and the fact that moisture and vapour are forced out of the chip in order to level out the pressure from 2 to 1 bar. After only a few seconds, however, the drying rate decreases rapidly and approaches a constant drying rate according to the new external conditions. The undisturbed drying rate curve is also depicted in Fig. 13 and intersects the other curves after about 5 s. Assuming the velocity of the chip in the dryer to be about 10 m s^{-1}, the post-drying effect corresponds to about 50 m of dryer length; this reduces the capital cost of the dryer significantly. Since the pressure of the steam inside the dryer as well as the dimensions of the wood chip are expected to influence the post-drying effect, some runs where these features were varied were performed also. The results are displayed in Table 2.

There is no difference evident between the two different exit times, although the post-drying effect is somewhat less for a larger chip. The effect of increasing the pressure is more pronounced and the post-drying effect is more than doubled when the pressure difference is increased from 1 to 2 bar. This is explained by increased flashing as the pressure difference between the conditions inside and outside the dryer increases.

5. THE EFFECT OF EXTERNAL PARTICLE HEAT TRANSFER

One important design parameter in a pneumatic conveying dryer is the heat transfer coefficient between the chip and surrounding steam. It is difficult to estimate this parameter both theoretically and experimentally since the chips are irregularly shaped and flow in an irregular manner. Several additional runs

Table 2. The post-drying effect under different conditions

Dimensions (mm)	Pressure (bar)	Exit time (s)	dX	Effect (s)
40; 4	2	30	0.02	5
40; 4	2	40	0.02	4.5
40; 4	3	40	0.04	11
40; 4	4	40	0.07	16
30; 3	2	30	0.03	3.5

for drying of spruce at 2 bar and 170°C with different slip velocities were performed. The results are displayed in Fig. 14, where the total drying time and the length of the constant drying rate period are plotted against the slip velocity. The results are normalised with respect to the velocity of 1 m s^{-1}.

It can be seen from Fig. 14 that the total drying time and the length of the constant rate period decrease rapidly as the slip velocity is increased from 1 to about 5 m s^{-1}. The decline thereafter is considerably slower. No constant rate period can be seen above about 10 m s^{-1}, which means that the whole drying sequence is controlled by internal resistance to mass and heat transport. As the velocities become very high (above 100 m s^{-1}), the total drying time approaches an asymptotic value of about 20% of the drying time at 1 m s^{-1}.

It may be concluded that, since drying is controlled by internal mass transfer during the main part of the drying sequence, an error in the heat transfer coefficient is not expected to affect the total drying time significantly. The heat transfer coefficient was adjusted both upwards and downwards by a factor of 25% in order to investigate this; the results are displayed in Fig. 15.

It is seen from Fig. 15 that the drying time is increased by about 14% when the heat transfer coefficient is reduced by 25%. For an increase of 25%, however, the drying time is only about 8% shorter. This indicates that drying, in these cases, is mainly controlled by internal transport.

One important result of the calculations in this section is the maximum size of a wood chip which is suitable for drying in a pneumatic conveying dryer. Assuming the heat transfer rate is high enough so that internal transport controls the entire drying sequence, the minimum residence time required to reach any desired moisture content can be determined. The chip is not suitable for drying in this type of dryer if this time exceeds about 40 s. Permeability also affects this result, so the same calculations using permeabilities valid for spruce wood were also performed. The

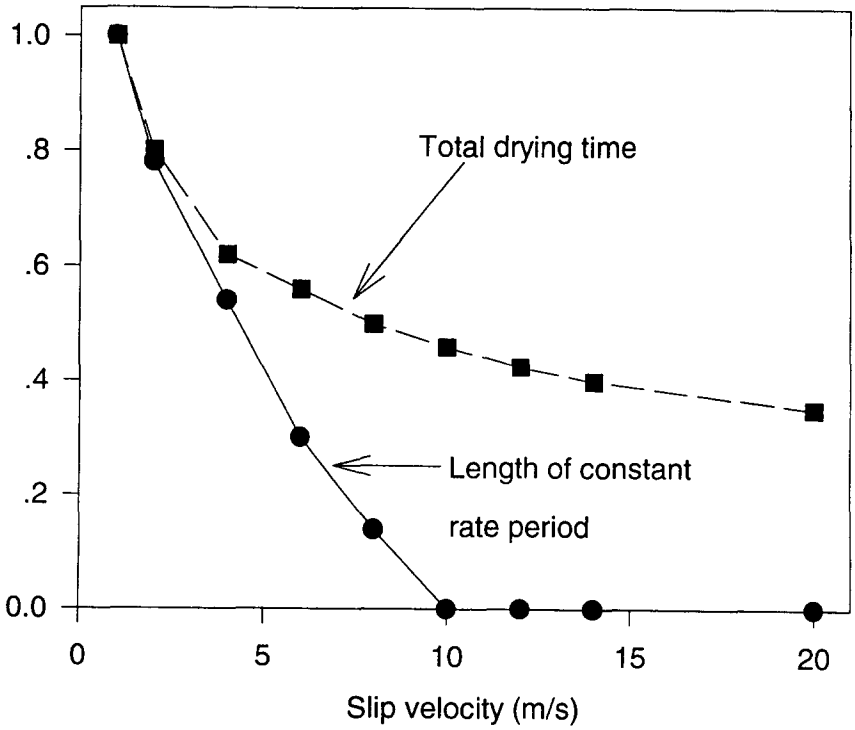

Fig. 14. Drying time as a function of the slip velocity.

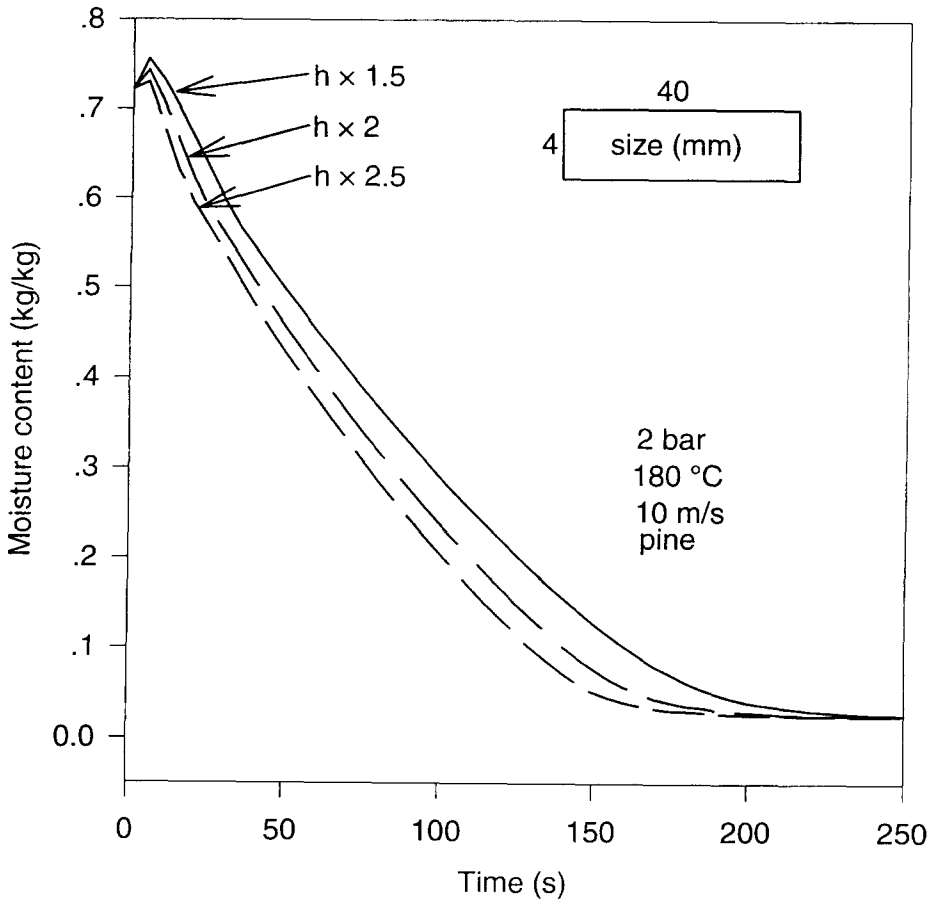

Fig. 15. The effect of the heat transfer coefficient.

results for two different wood chip sizes are displayed in Table 3.

It can be concluded from Table 3 that chips with the dimensions L, $T = 30$, 3 mm may be dried in this type of dryer, whereas it is impossible to reach moisture contents below 0.4 with chips any larger. The difference in drying time between the different wood species is rather large, since the internal resistance to mass transport is the dominating parameter.

It should be mentioned that the residence time can be increased by means of recirculation, thus allowing for larger particles to be dried in a pneumatic conveying dryer. The recirculation can be accomplished by inserting a separation device at the outlet. The output stream is split into two streams: one product stream and one which joins the feed. By utilising the difference in density between wet and dry material, the separation device can be constructed in such a manner that only moist material is recirculated.

6. THE IMPORTANCE OF A TWO-DIMENSIONAL MODEL

It is of interest, from a design point of view, to consider whether or not a two-dimensional (2-D) drying model for particle drying kinetics is needed. It is clear from the preceding sections that several significant effects arise when the anisotropicity of wood is taken into account. These physical phenomena would not have been as evident in a one-dimensional (1-D) model. It must be remembered, however, that the most important feature is the overall drying rate. A com-

Table 3. Minimum residence time in a pneumatic conveying dryer

Dimensions (L, T) (mm)	Type of wood	Drying time to $X = 0.3$ (s)	Drying time to $X = 0.4$ (s)	Drying time to $X = 0.5$ (s)
30; 3	spruce	40	29	19
30; 3	pine	37	26	16
40; 4	spruce	86	62	42
40; 4	pine	60	42	27

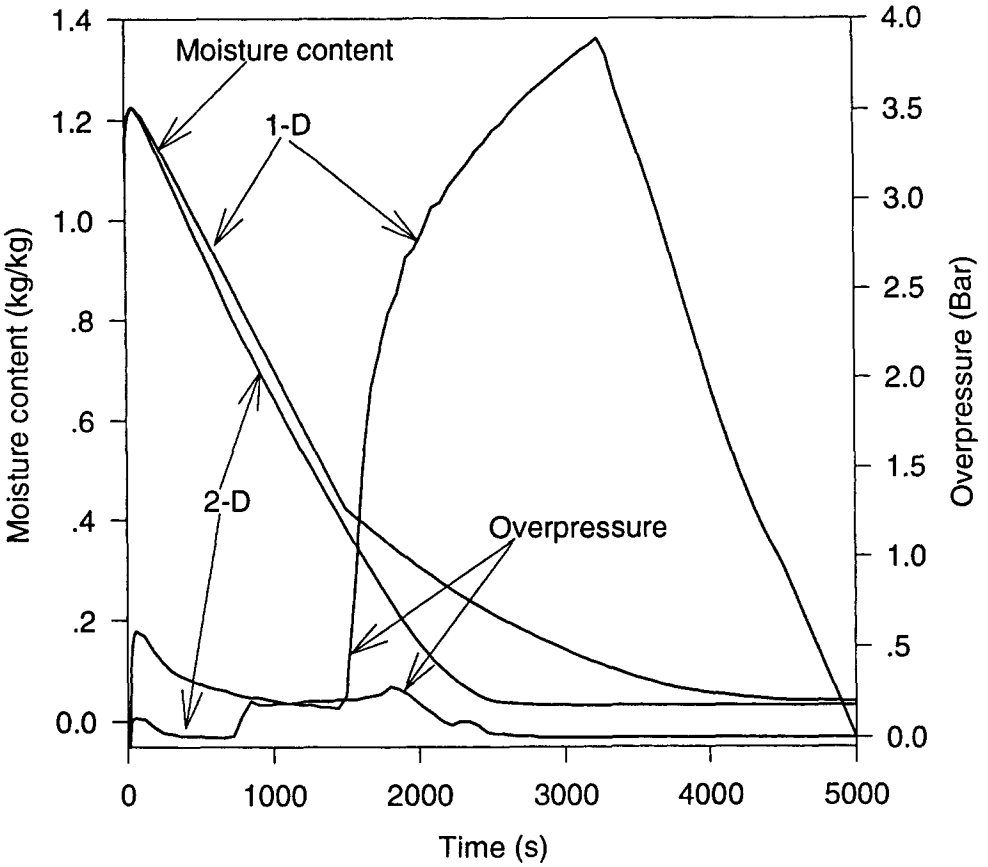

Fig. 16. Comparison between 1-D and 2-D drying.

parison between the behaviour of two-dimensional and one-dimensional (transversal) drying of spruce is depicted in Fig. 16. The dimensions of the wood chip and the external conditions are the same as in Fig. 2.

The drying rate is somewhat higher in the two-dimensional case, as shown in Fig. 16. The difference in drying rates in the constant rate period, is mainly due to the different sizes of the exchange surfaces (about 14% larger in the two dimensional case). The difference becomes greater in the later part of the drying since, in the two-dimensional case, the flow of vapour in the longitudinal direction contributes significantly to the drying rate. The overpressure becomes much greater in the one-dimensional case since no flow can occur in the more permeable direction. The overpressure is clearly overpredicted in the one-dimensional case and drying is considerably slower, which highlights the importance of a two-dimensional model.

An alternative way of illustrating the significance of allowing for flow in two directions is to compare the flow of water vapour and heat through each exchange surface: the results for the same drying case as in Fig. 16 are depicted in Fig. 17(a and b). The efflux of water vapour during the first 800 s, is mainly through the surface perpendicular to the transversal direction (the larger surface). The drying rate down to about 0.4 in average moisture content, consequently, is similar to that for a 2-D model.

Accordingly, it would suffice to use a 1-D model for the first part of the drying process. As the drying enters the falling rate period, the internal overpressure drives water vapour in the longitudinal direction. Consequently, from about 1000 s and onward, drying is controlled by the efflux of water vapour through the surface perpendicular to the longitudinal direction (the small surface). It should be noted that this surface is only about 14% of the size of the larger surface. The input flow of heat, on the other hand, is mainly through the larger surface during the whole drying process. The heat flow through the small surface is nearly constant during the entire drying sequence since the temperature at this surface is kept at the boiling point, as discussed above. To summarise, the transversal direction dominates the vapour efflux during the constant rate period of drying, while the longitudinal direction dominates during the later period of drying; about 90% of the total heat flow is in the transversal direction. It can be concluded that the effects of the two directions interact and that neither one of them can be disregarded without neglecting important features of the drying physics. It is also likely that an increase in the transversal permeability would make a two-dimensional simulation less neces-

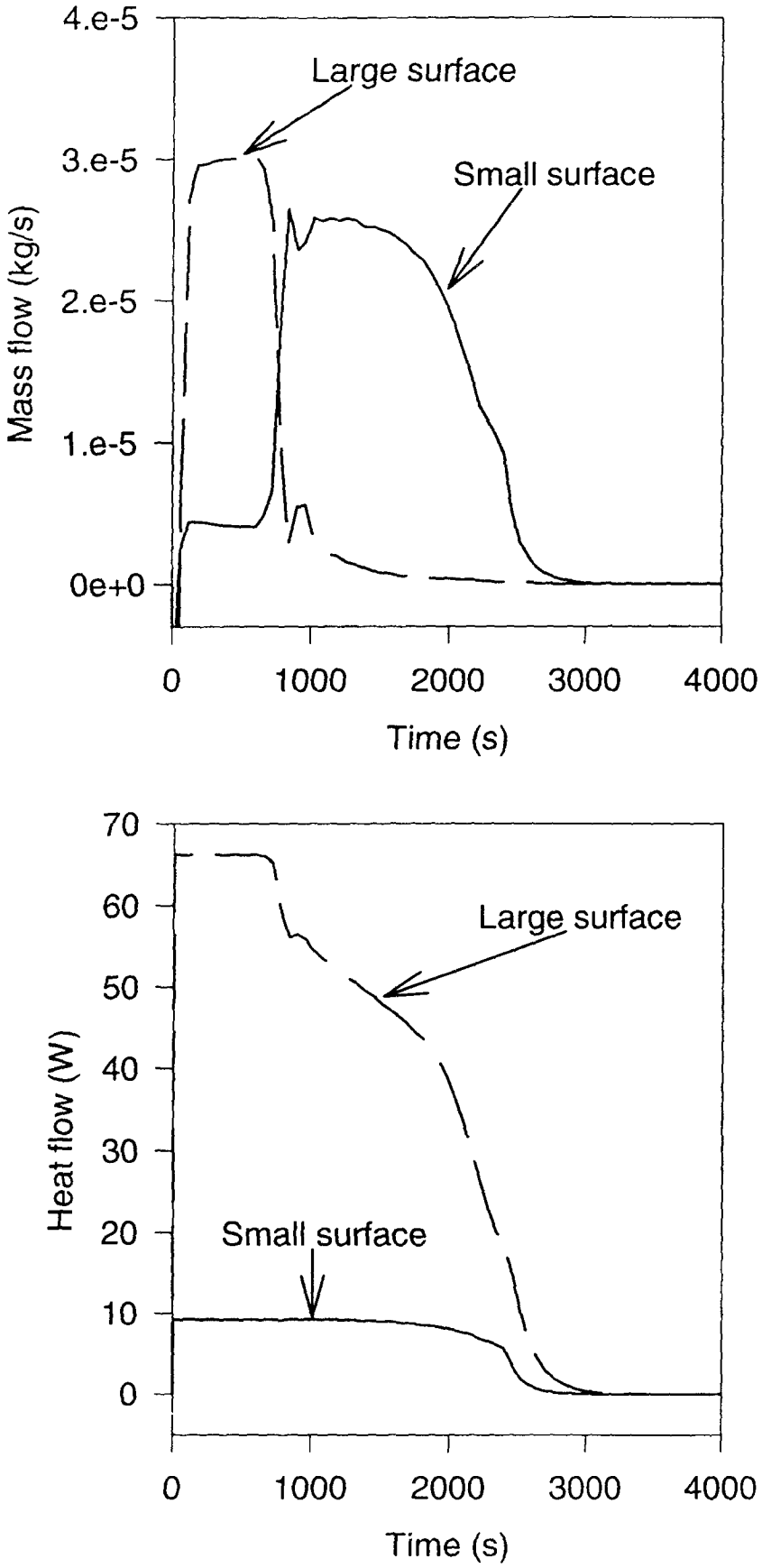

Fig. 17. The flow of vapour and heat through each exchange surface as a function of time.

sary, as drying will be controlled by flow in the transversal direction for a longer time. For the same reason, more permeable woods are less dependent on a two-dimensional model.

7. CONCLUSIONS

The difference in permeability between different wood species, or between different growth rates among samples of the same species, has a relatively minor effect on the total drying time under mild drying conditions. For more severe drying conditions, such as in a pneumatic conveying dryer, however, the difference in drying time between different species becomes more pronounced and must, therefore, be accounted for in the dimensioning of such a dryer.

It was found that the dimensions of the wood chip affected the drying time significantly. The total drying time increased approximately linearly with thickness as well as to the square root of the length. Accordingly, it can be stated that, while keeping the volume constant, the cutting of the wood chips should be carried out in such a manner that these geometrical constraints are taken into account.

Condensation of steam on the surface increases the drying time if the initial temperature of the chips is below the saturation point of the steam, which leads to poor utilisation of the drying equipment. This can be avoided by increasing the initial temperature of the chips through preheating, thereby decreasing the total drying time significantly.

Significant drying occurs after the dryer as a result of flashing (post drying). The effect of post drying is strongly enhanced by increased pressure inside the dryer. The exit time and dimensions of the wood chips have a minor influence on the post drying effect.

Under harsh drying conditions, such as in a pneumatic conveying dryer, the main part of the drying sequence is controlled by internal mass transfer. A small error in the predicted value of the external heat transfer coefficient has a limited effect on the total drying time. By inserting a very high value for the convective heat transfer coefficient, the minimum residence time for a specified chip can be calculated. It was found that chips thinner than 4 mm were suitable for drying in a pneumatic dryer only.

The main input of heat during the whole drying sequence is through the large surface perpendicular to the transversal direction, even though a significant portion of the net efflux of water is through the small surface perpendicular to the more permeable longitudinal direction. The features mentioned above can be assigned to the strong anisotropicity for wood which makes a two-dimensional model necessary.

REFERENCES

1. Mujumdar, A. S., Superheated steam drying: principles, practice and potential for use of electricity. Report no 817 U 671, Canadian Electrical Association, Montreal, Quebec, 1990.
2. Fyhr, C. and Rasmuson, A., Mathematical model of superheated steam drying of wood chips and other hygroscopic porous media. *AIChE Journal*, 1996, **42**, 2491–2502.
3. Pruess, K., TOUGH user's guide, Lawrence Berkeley Laboratory, University of California, Berkeley, CA, 1987.
4. Siau, J. F., *Transport Processes in Wood*. Springer, Berlin, 1984.
5. Johansson, A., Fyhr, C. and Rasmuson, A., High temperature drying of wood chips with air and superheated steam. *International Journal of Heat and Mass Transfer*, 1997, **40**, 2843–2858.
6. Perré, P., Moser, M. and Martin, M., Advances in transport phenomena during convective drying with superheated steam and moist air. *International Journal of Heat and Mass Transfer*, 1993, **36**, 2725–2746.
7. Björk, H. and Rasmuson, A., Moisture equilibrium of wood and bark chips in superheated steam. *Fuel*, 1995, **74**, 1887–1890.
8. Sorensen, A., Mass transfer coefficients on truncated slabs. *Chemical Engineering Science*, 1969, **24**, 1445–1460.

APPENDIX

Mathematical model

The wood contains free water above X_{fsp} as

$$X_l = X - X_{fsp}$$

where

$$X_{fsp} = 0.598 - 0.001T \text{ [4]}.$$

Balance equations

Mass

$$\frac{\partial M^\kappa}{\partial t} = \nabla \cdot \left(\sum_{\alpha=l,g} \mathbf{n}_\alpha x_\alpha^\kappa \right)$$

where

$$M^\kappa = \varepsilon \sum_{\alpha=l,g} S_\alpha \rho_\alpha x_\alpha^\kappa$$

where the relation between the moisture content X and liquid saturation S_l is written as:

$$X = \frac{S_l \varepsilon \rho_l}{(1-\varepsilon)\rho_{wood}}.$$

Heat

$$\frac{\partial H}{\partial t} = \nabla \cdot \mathbf{q}$$

where

$$H = (1-\varepsilon)\rho_{wood} C_{pwood} T + \varepsilon \sum_{\alpha=l,g} S_\alpha \rho_\alpha u_\alpha$$

$$\rho_{wood} = 1500 \text{ kg m}^{-3} \quad C_{pwood} = 1400 \text{ J kg}^{-1} \text{ K}^{-1}.$$

Porosity for soft wood $\varepsilon = 0.73$,
porosity for dense wood $\varepsilon = 0.67$.

Internal mass transfer

Convection according to Darcy's law

$$\mathbf{n}_\alpha = -\rho_\alpha \frac{k_\alpha}{\mu_\alpha} K_\alpha \nabla P_\alpha.$$

Relative permeabilities [6]

$$k_{l,T} = X^{*3} \quad \text{with} \quad X^* = \frac{X_l}{X_{sat}}$$

$$k_{g,T} = 1 + (2X^* - 3)X^{*2}$$

$$k_{l,L} = X^{*8}$$

$$k_{g,L} = 1 + (4X^* - 5)X^{*4}.$$

Absolute permeabilities [4] (m^2)

$$\text{spruce} \quad K_{l,T} = 5 \times 10^{-17}, \quad K_{l,L} = 5 \times 10^{-13}$$

$$\text{pine} \quad K_{l,T} = 2.5 \times 10^{-16}, \quad K_{l,L} = 1 \times 10^{-12}$$

$$K_g = 0.1 \times K_l \quad \text{(pit aspiration)}.$$

The liquid and gas pressures are coupled as:

$$P_l = P_g - P_c$$

where P_c is the capillary pressure [6]:

$$P_c = 1.364 \times 10^5 \sigma (X_l + 1.2 \times 10^{-3})^{-0.63}.$$

Bound water diffusion [4]:

$$\mathbf{n}_l^w = -D_{bw} \nabla X$$

$$D_{bw,T} = 0.05 D_{BT} / ((1 - a^2)(1 - a))$$

$$D_{BT} = 7 \times 10^{-2} \exp(-(9200 - 7000X)/RT)$$

$$a^2 = 1 - 0.5(\varepsilon + X) \quad R = 1.987 \text{ kcal mol}^{-1} \text{K}^{-1}$$

$$D_{bw,L} = D_{bw,T} 250 a^2.$$

Gas diffusion coefficient in equation (4) [6]:

$$D_{eff,T} = k_g D_v / 1000$$

where D_v is the diffusion coefficient of vapour in air

$$D_{eff,L} = 20 D_{eff,T}.$$

Internal heat transfer (convection + conduction)

$$\mathbf{q} = \sum_{\alpha = l,g} (\mathbf{n}_\alpha H_\alpha) - \lambda \nabla T.$$

Conductivity [6]

$$X \geqslant 0.4, \quad \lambda_T = (0.65/100X + 0.0932) \times (1 + 3.65 \times 10^{-3} T)(0.986 + 2.695X)$$

$$X \leqslant 0.4, \quad \lambda_T = (0.129 - 0.049X)(1 + (2.05 + 4X) \times 10^{-3} T) \times (0.986 + 2.695X)$$

$$\lambda_L = 2.5 \lambda_T \quad (T \text{ in } ^\circ C).$$

Vapour pressure lowering [7]:

$$P_v = \theta P_{v,sat}$$

$$\theta = D + \sqrt{D^2 + A/B}$$

$$A = -9.94 + 2.45/X_{fsp}, \quad B = 58.17 - 7.69/X_{fsp}$$

$$C = 68.08 - 9.15/X_{fsp}, \quad D = -0.5(1/CX - C/B).$$

Boundary conditions

Mass

$$P|_s = P_\infty$$

This pressure condition is realized by setting very high permeabilities at the surface. Gas is allowed to cross the surface only. In the case of air in the surroundings, the additional mass transfer condition is:

$$n_g^w|_s = k_c \frac{M_w P}{RT} (y_{w,s} - y_{w,\infty}).$$

Heat

$$q|_s = h(T_\infty - T_s) + \sigma_B e (T_\infty^4 - T_s^4) + \mathbf{n}_g H_g$$

where the emissivity, e, is set to 0.9.

Heat transfer coefficient [8]

$$h = 0.106 v_\infty \rho_f C_{Pf} Re_L^{-0.25}.$$